Capillary Bridges between Two Spherical Bodies

ARTICLE *in* LANGMUIR · OCTOBER 2000

Impact Factor: 4.46 · DOI: 10.1021/la000657y

Capillary Bridges between Two Spherical Bodies

Christopher D. Willett,*,† Michael J. Adams,‡ Simon A. Johnson,‡ and Jonathan P. K. Seville†

School of Chemical Engineering, The University of Birmingham, Edgbaston, Birmingham, B15 2TT, U.K., and Unilever Research Port Sunlight, Bebington, Wirral, Merseyside, CH63 3JW, U.K.

Received May 8, 2000. In Final Form: August 9, 2000

A method was developed for measuring the capillary forces arising from microscopic pendular liquid bridges. Results are described for perfectly wetting bridges between spheres of equal and unequal radii. A comparison with the theoretical values calculated from a numerical integration of the Laplace−Young equation demonstrated the accuracy of the method. It also showed that existing criteria for gravitational distortion are too restrictive and that the influence of the disjoining pressure is negligible. The Derjaguin approximation for spheres of unequal size was shown to be relatively accurate for small bridge volumes and for separation distances excluding those at close-contact and near-rupture, which correspond to maxima in the filling angle. Closed-form approximations were developed in order to conveniently calculate the capillary forces between equal and unequal spheres as a function of the separation distance and for a given bridge volume and contact angle. A closed-form approximation was also developed to calculate the rupture distance for liquid bridges between spheres of unequal sizes.

Introduction

There has been a resurgence of interest in the capillary forces between two solid bodies connected by a pendular liquid bridge. This has arisen from a recognition of the effects of moisture condensation at nanocontacts, which has a number of ramifications as pointed out recently by Gao.[1] These include their influence on both the normal and tangential forces obtained from scanning probe instruments[2−4] and also the performance of magnetic hard-disk devices.[5] However, the importance of the effects of the capillary forces in many industrial processes has long been recognized. A typical example is their role in particle size enlargement processes[6] that involve the growth of wet agglomerates. Recently, discrete computational procedures have been developed[7,8] in order to simulate the mechanical behavior of agglomerates during the types of collision that occur in such processes. These procedures require an efficient algorithm for representing the influence of the capillary forces.

A capillary junction between two solid bodies is termed a "pendular liquid bridge"; in the current paper, axisymmetric bridges between spheres will be considered. The capillary forces originate from the axial component of the surface tension acting at the liquid−gas interface and the Laplace hydrostatic pressure in the interior of a bridge. The former component is positive and attractive. The Laplace pressure component is proportional to the curvature of the bridge surface and can be repulsive or attractive. An attractive contribution to the total capillary force occurs if the Laplace pressure is negative. This is the case if the bridge surface curvature is negative with respect to the interior of the bridge.

Starting with the early work of Haines[9] and Fisher,[10] many papers have reported calculations of capillary forces. It has been shown that there is a dependence on the separation distance of the solid bodies; the surface tension, geometry, and volume of the liquid bridge; and the contact angles that the liquid makes with the solid surfaces. One of the most comprehensive studies is due to Orr et al.[11] who solved the Laplace−Young equation analytically in terms of elliptic integrals. They also considered the gravitational distortion of the meniscus profile but, for the length scales associated with the applications described above, the effect is generally insignificant. More recently, Gao[1] has provided solutions that take into account the surface interactions and liquid evaporation. In particular, he emphasized that there are three types of boundary conditions, depending on whether the liquid perfectly wets either or both the solid surfaces. The earlier work, for example by Orr et al.,[11] was strictly applicable to cases where the liquid did not wet the solid surfaces. Under wetting conditions, there exists an equilibrium between the disjoining pressure in the liquid film on the wetted surfaces and the hydrostatic pressure in the liquid bridge. Gao et al.[1,12] calculated the total capillary force from the derivative of the total interfacial free energy with respect to the separation distance. It was shown that the contribution to the capillary force of the surface interactions, due to the disjoining pressure, is small for systems involving spherical bodies when the equatorial diameter of the bridge is small relative to the sphere radius and the separation distance is much less than that corresponding to rupture. This is not the case for a bridge

* Corresponding author. Present address: Unilever Research Port Sunlight. E-mail: Christopher.Willett@unilever.com.
† The University of Birmingham.
‡ Unilever Research Port Sunlight.

(1) Gao, C. *Appl. Phys. Lett.* **1997**, *71*, 1801.
(2) Piner, R. D.; Mirkin, C. A. *Langmuir* **1997**, *13*, 6864.
(3) Crassous, J.; Charlaix, E.; Loubet, J. L. *Phys. Rev. Lett.* **1997**, *78*, 2425.
(4) Shao, Z.; Gao, C.; Yuan, J.-Y. *Mod. Phys. Lett.* **1992**, *B6*, 9.
(5) Gao, C.; Bhushan, B. *Wear* **1995**, *190*, 60.
(6) Seville, J. P. K.; Tüzün, U.; Clift, R. *Processing of Particulate Solids*; Kluwer Academic Publishers: Dordrecht, 1997.
(7) Thornton, C.; Yin, K. K.; Adams, M. J. *J. Phys. D: Applied Phys.* **1996**, *29*, 424.
(8) Mikami, T.; Kamiya, H.; Horio, M. *Chem. Eng. Sci.* **1998**, *53*, 1927.
(9) Haines, W. B. *J. Agric. Sci.* **1925**, *15*, 529.
(10) Fisher, R. A. *J. Agric. Sci.* **1926**, *16*, 492.
(11) Orr, F. M.; Scriven, L. E.; Rivas, A. P. *J. Fluid Mech.* **1975**, *67*, 723.
(12) Gao, C.; Dai, P.; Homola, A.; Weiss, J. *ASME J. Tribol.* **1998**, *120*, 358.

10.1021/la000657y CCC: $19.00
Published on Web 10/21/2000

between a cone and a planar surface where the disjoining pressure has a significant effect on the total capillary force.[12]

In addition to the calculation of the magnitude of the capillary forces, there have been studies of the stability of pendular bridges. A numerical evaluation of the Laplace−Young equation results in two solution branches that converge to a single solution at a critical separation distance. Erle et al.[13] argued that this solution corresponded to the rupture distance when the solution was formulated in terms of the bridge neck diameter. De Bisschop and Rigole[14] used the minimum in the filling angle, which resulted in a significant underestimation of the rupture distance. Lian et al.[15] expressed the solution in terms of the minimum free energy, which allowed the more stable branch to be identified. They also showed that the rupture distance calculated by this procedure was equal to the values obtained by expressing the solution in terms of the filling angle, the neck diameter, and the force. In the current paper, we are investigating the force and rupture behavior. Consequently, it was convenient to employ the force to obtain the rupture distance.

Although the Laplace−Young equation provides an exact solution for the hydrostatic component of the total capillary force and also the rupture distance, it is cumbersome for the routine interpretation of experimental data, and the algorithms involved are computationally expensive for implementing in the many-body simulations of the type mentioned previously.[7] Consequently, approximate solution procedures or approximate descriptions of the exact solutions, which may be expressed in closed-form, have been developed. The simplest approximation is to treat the meridional profile of a pendular bridge as a segment of a circle; Haines[9] originally proposed this "toroidal approximation". The errors associated with estimating the liquid bridge volume and capillary forces have been examined by a number of workers, including Orr et al.[11] and Mehrotra and Sastry.[16] Generally, they are quite small (<10%) for relatively small separation distances and bridge volumes. A well-known example of a toroidal solution is due to McFarlane and Tabor,[17] who derived a simple approximation for a sphere in contact with a flat surface. Based on more detailed toroidal calculations, Marmur[18] showed that this classical equation was of limited applicability.

The capillary attraction or repulsion between two solid surfaces is equal to the sum of the capillary forces acting across any plane that is orthogonal to the axis of symmetry joining the solid surfaces. The total force depends, as indicated above, on the curvature of the bridge surface. In the toroidal approximation, the surface curvature is not constant along the meridional profile of the bridge. Thus, the toroidal solution for the total force is a function of the local value of the surface curvature and hence the position of the orthogonal plane. The "gorge" method seems to provide the most accurate estimate of the capillary forces; the method refers to the solution evaluated at the neck of the bridge (in preference to evaluation at the three-phase contact line, for example).[19] This conclusion has been verified by Lian et al.,[15] who also made a significant improvement in the method by introducing simple scaling coefficients.

The application of the toroidal approximation to spheres of an unequal size involves more complex expressions compared to the case for equal spheres.[16] A simpler approach for calculating the capillary forces is to use the Derjaguin approximation.[20] This enables the expression for two equal spheres of radius R to be used with the substitution of the harmonic mean sphere radius, $R_{1,2}$, thus:

$$\frac{1}{R_{1,2}} = \frac{1}{2}\left(\frac{1}{R_1} + \frac{1}{R_2}\right) \tag{1}$$

where R_1 and R_2 are the radii of the two spheres. However, to the authors' knowledge, a systematic estimate of any errors involved with simply substituting R by $R_{1,2}$ has not been carried out.

For experimental or computational studies involving nonvolatile liquids, such that the volume of a liquid bridge is conserved, there is often a need to determine the total capillary force as a function of the separation distance. The point-wise calculations involved represent a significant disadvantage of the toroidal approximation. Nevertheless, de Lazzer et al.[21] have made significant progress with this approach, although the errors associated with their method increase with increasing separation distance.

Lian et al.[15] examined the functional behavior of the rupture distance for equal spheres calculated numerically as described previously. They found that this critical separation distance, $2S_c$, was proportional to the cube root of the volume of the liquid bridge, V:

$$\frac{2S_c}{V^{1/3}} = \frac{2S_c^*}{V^{*1/3}} = \left(1 + \frac{\varphi}{2}\right) \tag{2}$$

where $2S_c^*$ (= $2S_c/R$) and V^* (= V/R^3) are the dimensionless rupture distance and volume, respectively, and where φ is the contact angle. No satisfactory physical explanation for this rather simple relationship has yet been made.

Few papers report experimental data for the capillary forces with the necessary information for making comparisons with theory. The most comprehensive study is due to Mason and Clark.[22] They measured the total attractive force as a function of the separation distance between two equal spheres and between a sphere and plate for different bridge volumes. To obtain neutral buoyancy, the measurements were performed with the liquid bridge immersed in a second immiscible fluid having the same density. A detailed comparison of these data with the calculated values was made by Lian et al.[15] and it was found that the discrepancies, which ranged between ca. 0 and 20%, increased with decreasing separation distance and increasing bridge volume. A more limited comparison was made by Erle et al.[13] who also commented on the errors at small separation distances. They considered that their results were more consistent with those of Cross and Picknett,[23] who measured the force between equal spheres and also a sphere and plate at a zero separation distance and for a range of bridge volumes. They obtained a close agreement with theory for a zero contact angle, but the comparison was relatively poor for

(13) Erle, M. A.; Dyson, D. C.; Morrow, N. R. *AIChE J.* **1971**, *17*, 115.
(14) De Bisschop, F. R. E.; Rigole, W. J. L. *J. Colloid Interface Sci.* **1982**, *88*, 117.
(15) Lian, G.; Thornton, C.; Adams, M. J. *J. Colloid Interface Sci.* **1993**, *161*, 138.
(16) Mehrotra, V. P.; Sastry, K. V. S. *Powder Technol.* **1980**, *25*, 203.
(17) McFarlane, J. S.; Tabor, D. *Proc. R. Soc.* **1950**, *A 202*, 224.
(18) Marmur, A. *Langmuir* **1993**, *9*, 1922.
(19) Hotta, K.; Takeda, K.; Iinoya, K. *Powder Technol.* **1974**, *10*, 231.
(20) Israelachvili, J. N. *Intermolecular & Surface Forces*; Academic Press: London, 1992.
(21) de Lazzer, A.; Dreyer, M.; Rath, H. J. *Langmuir* **1999**, *15*, 4551.
(22) Mason, G.; Clark, W. C. *Chem. Eng. Sci.* **1965**, *20*, 859.
(23) Cross, N. L.; Picknett, R. G. In *Proceedings of the International Conference on the Mechanism of Corrosion by Fuel Impurities*; Johnson, H. R., Littler, D. J., Eds.; Butterworths: London, 1963; p 383.

a contact angle of 40°, with the error being ca. 30% for the greatest volume examined. Such adhesion measurements have been reported by McFarlane and Tabor[17] for macroscopic contacts and also by Fisher and Israelachvili[24] using a surface force apparatus. Hotta et al.[19] measured the forces between spheres and the surface of water and spheres and a flat glass plate for a range of separation distances. Their results for a sphere interacting with a free surface of water showed agreement with theory to within 10%. However, for the sphere-on-flat arrangement, there was a considerable reduction in the attractive force at close contact. A similar result was obtained by Mason and Clark[22] and is not consistent with theory. Mazzone et al.[25] measured the forces between two steel spheres for a range of separation distances and bridge volumes, using dibutylphthalate as the liquid. This had a contact angle of 10° with the steel. Interestingly, they also found a similar deviation from theory for close contact, as was observed by Mason and Clarke[22] and Hotta et al.[19]

Mason and Clark[22] measured the rupture distances as a function of the bridge volume. These data are reasonably consistent with the values calculated using eq 2 on the basis of the stability analysis described above.[15] Fairbrother and Simons[26] also measured the rupture distances between equal spheres for contact angles of 0°, 34°, and 50°. They compared the data with those calculated using the expression developed by Lian et al.,[15] and the agreement was within ca. 10%.

In summary, the capillary forces and rupture distances associated with axisymmetric pendular liquid bridges may be calculated by a numerical integration of the Laplace−Young equation. Mason and Clark[22] have carried out the only systematic experimental study of the capillary forces for a range of separation distances and bridge volumes. This work was restricted to equal spheres and a sphere and flat and was for a near perfectly wetting fluid. Furthermore, there were significant discrepancies with theory. The limited experimental studies reflect the difficulties in measuring the small forces and length scales associated with bridges that are sufficiently small that gravitational distortion is insignificant. The current paper describes equipment that was developed to allow such measurements to be made both conveniently and accurately. Relatively simple systems are examined that may be compared with theory in order to establish the accuracy of the method. In particular, bridges with a zero contact angle were examined in order to avoid the complication of wetting hysteresis. However, the systems include spheres of unequal size that have not been studied previously. Closed-form approximate expressions were also developed in the current work that are valuable for interpreting experimental data and for the efficient implementation of many-body simulations involving capillary bridges.

Experimental Section

Equipment. To measure the attractive force due to a liquid bridge between either a pair of spheres or a sphere and a flat plate, a sphere was, in both cases, attached to a sensitive microbalance (MK2 vacuum head with Multicard II controller, CI Electronics Ltd., Salisbury, U.K.). The analogue output of the microbalance was connected to a PC data logging system, which continuously recorded the apparent weight of this "upper" sphere: the noise on this force measurement was 300 nN peak-to-peak for data averaged over 20 ms. The value of the force averaged over a period of five seconds remained within bands 15 nN and 100 nN wide over two minutes and 3 h, respectively. The smaller of these two values determined the precision with which liquid drops could be weighed. The position of the microbalance, and hence the upper sphere, in the vertical (Z) direction could be adjusted using a micromotion stage to which a manual micrometer, with a digital display, was attached. This had a setting resolution of 1 μm.

The "lower" sphere, or flat, was attached to the upper surface of a piezoelectric actuator (17 PAZ 015 piezoelectric actuator with feedback and a 17 PAZ 001 piezoelectic controller with feedback, Melles Griot Ltd., Cambridge, U.K.) for accurate positioning in the Z direction. The piezo-actuator was mounted on an XY micromotion stage to enable the precise alignment of the lower sphere, or flat, in the horizontal plane. The piezo-actuator had a setting resolution and peak-to-peak noise of 10 nm, an internal mean positional stability of ca. 1 nm, and a maximum stroke length of 100 μm. The displacement of the piezo-actuator, and therefore the fine control of the separation between the solid surfaces, results from the potential difference across it, which could be changed either locally using the control unit or remotely under computer control. The latter facility provided a linearly increasing voltage with time in order to achieve a constant approach/separation velocity. The resulting motion was free of any directional hysteresis due to the use of closed-loop feedback from a displacement transducer inside the actuator.

The central gap between the solid surfaces was not directly measured but was inferred from the Z-stage micrometer reading, the piezo-actuator position, and the values of these parameters at the point of solid−solid contact. This assumes that the position of the microbalance arm was independent of the force applied to it. This was verified using an optical noncontact displacement transducer (Rodenstock laser stylus LS10, Mahr U.K. Plc., Milton Keynes, U.K.) focused on the upper surface of the arm of the microbalance. The movement was found to be negligible for forces that varied slowly with time or with separation distance in liquid bridge experiments done at relatively small, and constant, approach or separation velocities. However, rapid changes in force did lead to some movement, since the PID control loop maintaining the position of the balance arm could not respond sufficiently fast. As an example, a 300 μN step reduction in load resulted in an arm-end movement of ca. 65 μm in 100 ms. A further 5 s was required for the balance arm to recover its initial position. Despite this, the force reading stepped down with negligible overshoot and stabilized within 100 ms. Thus, the dynamics of the microbalance limited force measurements to relatively small separation velocities in order to eliminate uncertainties in the instantaneous separation distance.

The alignment of the sphere (and also the recording of bridge profiles and volumes) was facilitated by the use of a horizontally orientated video microscope (Infinivar, Parfocal Ltd., Ringwood, U.K.). The entire equipment was mounted on an antivibration table and enclosed in a draft-free box. Measurements were carried out in an environmentally controlled laboratory at 20 °C and at ca. 50% RH.

The data logger continuously recorded both the displacement of the actuator and the microbalance force, typically at an acquisition rate of 5 Hz. Suitable zero-point determination, under the operating conditions described above, enabled the capillary force to then be expressed as both a function of time and of the distance separating the two solid surfaces.

Materials. Precision synthetic sapphire spheres (Dejay Distribution Ltd., Wokingham, U.K.) were employed. The upper sphere had a radius of 2.381 mm, and the lower spheres had radii of 2.381, 1.588, and 1.191 mm in order to obtain radius ratios of unity, 2/3, and 1/2, respectively. In addition, a sapphire disk (Melles Griot Ltd., Cambridge, U.K.) was used as a lower flat surface for sphere−flat experiments. The spheres were manufactured to a high precision, the surfaces were very smooth, and the diameters were measured using a digital micrometer having a 1 μm resolution. The sapphire spheres and the flat were cleaned using alcohol (AnalaR grade, BDH Laboratory Supplies, Poole, U.K.), which was sufficient to obtain perfect wetting of the liquid used for the bridges. This was a DC200 poly (dimethylsiloxane) silicone fluid (Fluka Chemicals, Gillingham, U.K.). The

(24) Fisher, L. R.; Israelachvili J. N. *Colloids Surf.* **1981**, *3*, 303.
(25) Mazzone, D. N.; Tardos, G. I.; Pfeffer, R. *J. Colloid Interface Sci.* **1986**, *113*, 544.
(26) Fairbrother, R. J.; Simons, S. J. R. *Part. Part. Syst. Char.* **1998**, *15*, 16.

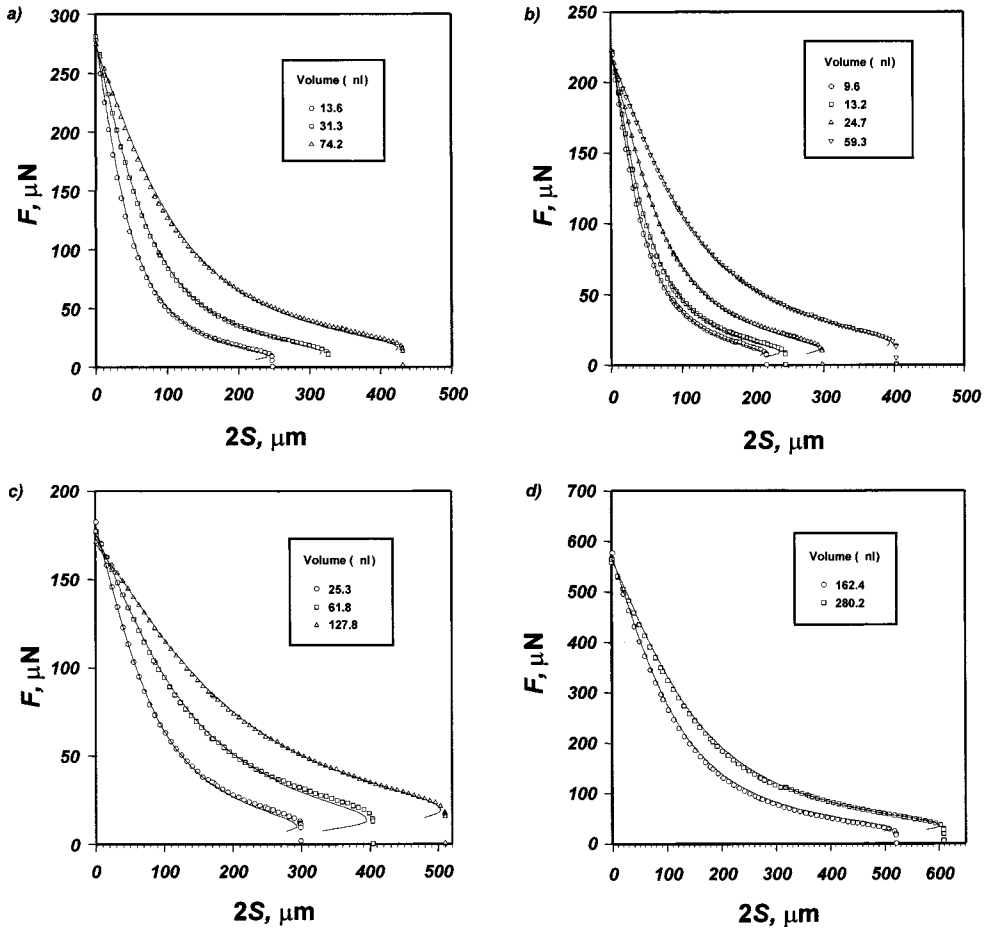

Figure 1. The measured total capillary force for a range of liquid bridge volumes as a function of the separation distance between two spheres, where the ratios of the radii are (a) 1, (b) 2/3, (c) 1/2, and (d) 0. The curves represent the values calculated by numerical solution of the Laplace−Young equation (for $\varphi = 0°$) and using eq 3.

measured viscosity, surface tension, and density of this fluid were 110 mPa·s, 20.6 mN/m, and 960 kg/m^3, respectively.

Measurement Procedure. For the measurements involving two spheres, the position of the lower sphere was adjusted using the *XY* micromotion stages until it was directly below the upper sphere, as shown by a reduction in the apparent weight of the latter when the vertical position of the balance was in suitable position. This alignment procedure was aided by the use of the video microscope that was focused on the lower part of the upper sphere. The contact point position could then be established by suitable adjustment of the piezo-actuator.

A small quantity of the test fluid was brought into contact with the base of the upper sphere using a hypodermic needle. Although it is possible to calculate the resulting liquid bridge volume from the mass of this drop, it was more convenient to analyze the video images of the pendular bridge subsequently in order to obtain this information; the accuracy of the two methods was similar for relatively large liquid bridges (see later). The upper sphere was lowered using the *Z* micrometer until the liquid bridge formed and the microbalance showed an increase in downward force. The piezo-actuator was then adjusted to decrease the gap between the spheres until solid−solid contact occurred, as indicated by a decrease in the force read by the microbalance. The video images captured at this point were used to determine the volume of the bridge.

To measure the total capillary force as a function of the separation distance, the lower sphere or flat was moved downward at a constant rate of 1 μm/s. The attractive force between the solid surfaces was recorded continuously by the PC data logger until the bridge ruptured. The attractive force due to viscous flow between two separating solid spherical surfaces is directly proportional to the separation velocity and inversely related to the separation distance in the case of a Newtonian fluid.[27] Consequently, there was a large initial step increase in the measured force when the motion was initiated, but the contribution from this decayed rapidly over separation distances of a few microns. For this reason, data obtained at separation distances of less than 5 μm were discarded. The maximum displacement of the piezo-actuator was 100 μm. For bridges having greater rupture distances, a number of different experiments were carried out starting at different separation distances that were selected by a suitable adjustment of the *Z* stage micrometer. The results were subsequently spliced together in order to derive the force−separation data for the full range of separations in excess of the maximum allowable by a single sweep of the piezo-actuator voltage.

The slow separation velocity of 1 μm/s was selected in order to ensure that dynamic surface tension or viscosity effects, and also the dynamics of the microbalance, did not interfere with the force measurements. This was confirmed by the repeatability of the measurements carried out at slower velocities. Moreover, the absence of force hysteresis during directional reversal was further evidence that there was no viscous contribution to the measured force for the 110 mPa·s silicone fluid used at separation distances greater than the minimum value of 5 μm.

The liquid bridge rupture distances were measured directly using the digital display on the *Z* micromotion stage micrometer. A bridge was carefully and slowly extended by a manual adjustment of the Z micromotion stage, and the separation distance was recorded after the bridge was observed to rupture. It was found that this technique enabled rupture distances to be estimated to within ±1 μm.

(27) Lian, G.; Adams, M. J.; Thornton, C. *J. Fluid Mech.* **1996**, *311*, 141.

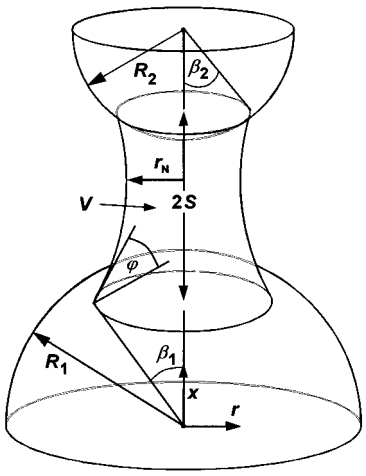

Figure 2. A schematic representation of a liquid bridge of volume V and surface tension γ between two spheres of radii R_1 and R_2 separated by a distance $2S$ with a neck radius r_N, a liquid−solid contact angle φ, and half-filling angles β_1 and β_2.

Results

Figure 1 shows the measured attractive forces as a function of the separation distance for different combinations of the spheres and also a sphere and flat. The results refer to different ratios of the radii of the spheres where, for the present purposes, the planar surface will be regarded as a sphere with a reciprocal radius of zero. For all configurations, it may be seen that there is a monotonic reduction in the force until bridge rupture occurs and no maxima were observed at close separation, as has previously been reported.[19,22,25]

To assess the accuracy of these results, comparisons were made with the theoretical values. The influence of the disjoining pressure was neglected for these calculations; this is reasonable for spherical bodies, as explained earlier. Figure 2 shows an axisymmetric liquid bridge between two unequal spheres. The liquid bridges studied in the current work exhibited a well-defined neck up to the point of rupture. The orthogonal plane passing through the neck at its minimum radius provides a convenient location, including the cases where the sizes of the spheres are unequal, for calculating the total downward force on the upper sphere, F, as follows:

$$F = 2\pi r_N \gamma - \pi r_N^2 \Delta P - V_s \rho g \qquad (3)$$

where γ and ρ are the surface tension and density of the liquid, respectively, r_N is the radius of the neck, ΔP is the hydrostatic pressure difference across the air−liquid interface, V_s is the volume of the upper sphere that is submerged in the liquid, and g is the acceleration due to gravity. The first term is the vertical component of the surface tension acting at the perimeter of the neck, and the second arises from the pressure difference acting on the cross-section of the neck. The third term is the buoyancy force, which was found to be negligibly small (<0.1%) for the range of bridges examined here.

The pressure difference and liquid bridge volume were obtained by numerical integration[19] of the Laplace−Young equation which may be written as follows:

$$\Delta P = \frac{\gamma}{\bar{r}} = \gamma\left[\frac{1}{r_1} + \frac{1}{r_2}\right] = \gamma\left[\frac{1}{r(1+\dot{r}^2)^{1/2}} - \frac{\ddot{r}}{(1+\dot{r}^2)^{3/2}}\right] \qquad (4)$$

where $\bar{r}$ is the radius of curvature of the bridge surface, $r(x)$ is the meridional bridge profile (see Figure 2), r_1 and r_2 are local principal radii of normal curvature in orthogonal directions at points along the meridional bridge profile, and the dot notation refers to differentiation with respect to x. Conventionally, r_1 is evaluated in a direction orthogonal to the meridional profile such that its center of curvature is located along the surface normal on the bridge axis of symmetry. Hence, the center of curvature of r_1 is always within the liquid bridge, or one of the spheres, and r_1 itself is positive and equals r_N when calculated at the neck. r_2 is evaluated in a direction containing the meridional bridge profile and can be positive or negative depending on whether its center of curvature lies inside or outside the liquid bridge, respectively. A negative $\bar{r}$ leads to a negative Laplace pressure and an attractive contribution to the total capillary force.

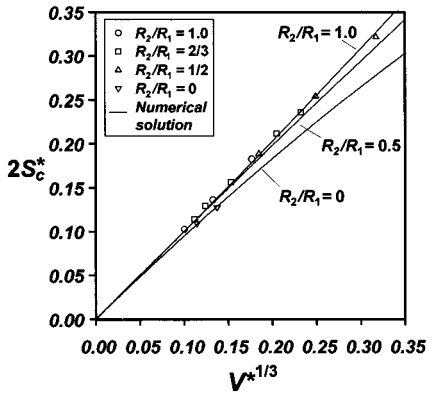

Figure 3. A dimensionless plot of the measured rupture distance as a function of the liquid bridge volume for spheres with different ratios of the radii; the curves represent the values calculated by numerical solution of the Laplace−Young equation (for $\varphi = 0°$).

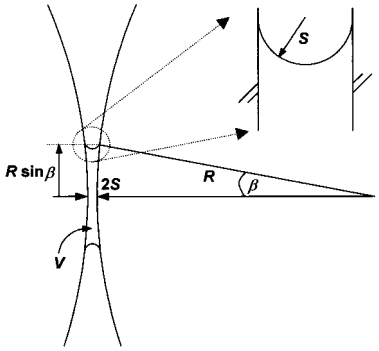

Figure 4. The geometry for small liquid bridges with a contact angle of zero between two equal spheres where the radius of curvature of the bridge surface is approximately given by the half-separation distance, S.

A correct, gravity-free, numerical solution results in a bridge profile with a constant surface curvature (= $1/\bar{r}$) that has a geometry consistent with the contact angle, the separation distance between the spheres, and the bridge volume. Some theoretical curves generated from such numerical solutions (for $\varphi = 0°$) are shown in Figure 1, and it can be seen that there is excellent agreement with the experimental data. More specifically, the root-mean-square deviation of the experimental data from the theoretical values for the aggregated data set is 3.7%; for the individual curves, the deviation is in the range 0.7−5.2%. As was described above, the measured bridge volumes were actually calculated from an analysis of the video images. Specifically, the neck radius for a known separation distance was measured and compared with that calculated by numerical simulation of the bridge profile. The bridge volume in this calculation was iterated

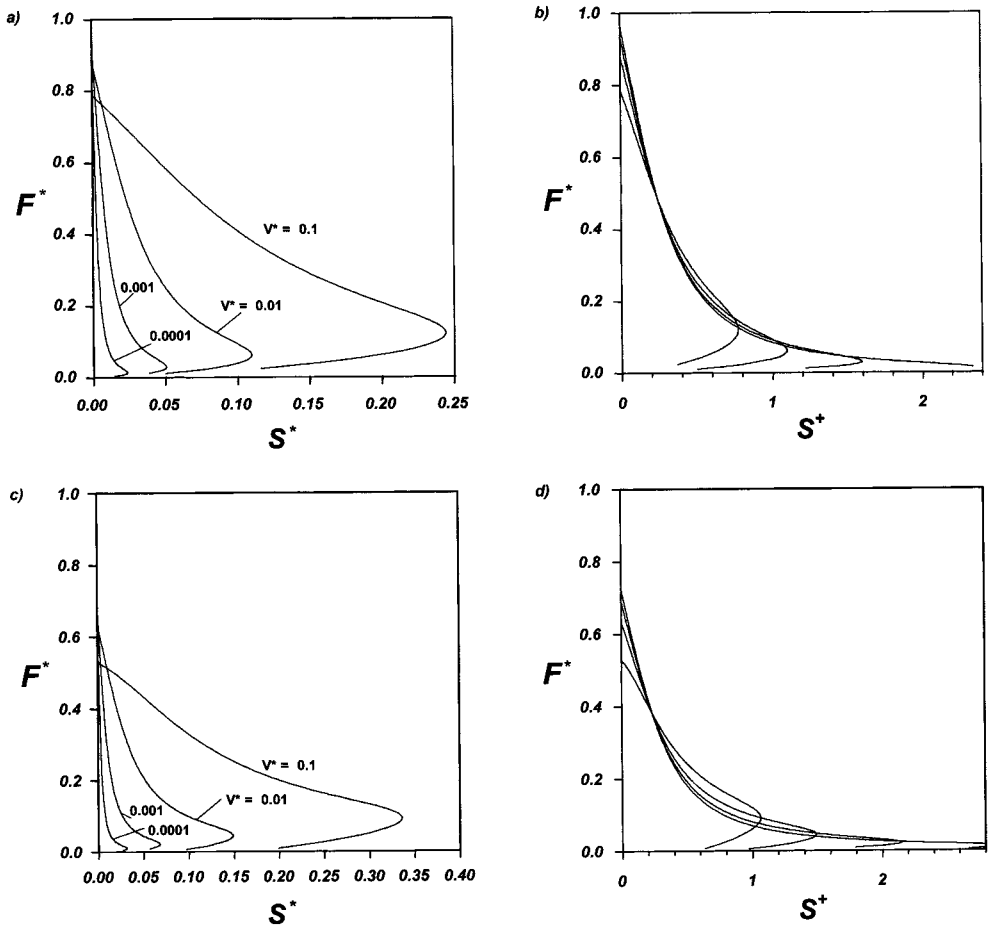

Figure 5. Dimensionless plots of the total capillary force as a function of the separation distance between equal spheres, calculated by numerical solution of the Laplace−Young equation and using eq 3. The contact angles are zero for (a) and (b), and 40° for (c) and (d).

until the difference in neck radius was <0.1%. This volume was found to be equal within 0.2% of that estimated from the mass of the liquid applied, at least for relatively large liquid bridges. As described in the previous section, the potential mass resolution of the microbalance was *ca.* 15 nN, which is equivalent to a liquid volume of 1.5 nL. Thus, for the smaller bridges, the resolution of the microbalance was insufficient for obtaining accurate values of the volume.

It was assumed that the influence of gravity was negligible in the above calculations, so that the pressure difference calculated for any particular bridge was independent of its orientation with respect to gravity. According to Princen,[28] it is not possible to specify a precise criterion for identifying the conditions under which gravitational distortion influences the magnitude of the capillary forces unless exact calculations are performed. He provides a conservative condition: $|\Delta P| \gg 2S\rho g$, where $2S$ is the distance separating the spheres (see Figure 2). On this basis, he has proposed two possible maximum values of the half-filling angle, β (see Figure 2), for a given Bond number ($Bo = \rho g R^2/\gamma$) that correspond to the gravity-free limit. For example, filling angle limits of 10° and 18° were proposed for a Bond number of 2.6. Mazzone et al.[25] proposed an alternative upper bound such that the Bond number should be less than unity.

Figure 3 is a dimensionless plot of the measured rupture distance as a function of the bridge volume for the cases given in Figure 1. The harmonic mean sphere radius, $R_{1,2}$, was used in order to calculate the dimensionless groups for bridges between unequal spheres (i.e., $2S_c^* = 2S_c/R_{1,2}$ and $V^* = V/R_{1,2}^3$). Figure 3 includes the exact values calculated (for $\varphi = 0°$) using eq 4, which for equal spheres show the functionality expected from eq 2. Furthermore, for a given dimensionless volume, the calculated dimensionless rupture distance decreases as the size ratio decreases. This is reasonably consistent with the experimental results.

Discussion

The capillary forces between spheres having equal and unequal radii were measured as a function of the separation distance. These data are consistent with the values calculated using the Laplace−Young equation. In particular, the smaller-than-expected forces at close contact, observed by a number of workers such as Mason and Clark,[22] were absent. Even though the solid−liquid contact angle was zero, the agreement with theory suggests that the influence of the disjoining pressure is negligible, as was predicted by Gao.[1,12] In addition, it suggests that the influence of gravitational distortion was negligible. Some of the liquid bridges contravened either or both the gravity-free limits[25,28] that were discussed in the previous section. Consequently, it may be reasonably concluded that such criteria are too conservative, as suggested by Princen.[28] Finally, the rupture distances were in close agreement with the values calculated using the expression developed by Lian et al.[15] except for those obtained from the sphere−flat combination. The calculated rupture distances show a small but significant monotonic reduction as the

(28) Princen, H. M. *J. Colloid Interface Sci.* **1968**, *26*, 249.

difference in the size of the spheres increases. In the remainder of this section, closed-form approximations for calculating the forces and rupture distances will be considered.

Closed-Form Expressions for Capillary Forces between Equal Spheres. One approach to developing a closed-form approximation for the capillary forces as a function of the separation distance, at a constant bridge volume, is to apply the principle of reduced variables. This requires a parameter for scaling the separation distance that will reduce the force−separation curves at different volumes to a single function. To identify an appropriate scaling parameter, an approximate model will be developed that has an analytical solution for the case of a small bridge with a zero contact angle between large spheres at a small separation distance. The errors in applying the superposition outside these limits will then be assessed.

Figure 4 shows such a pendular bridge between two equal spheres of radius R separated by a distance $2S$. To calculate the volume, a cylindrical geometry of radius $R\sin\beta$ is assumed:

$$V = 2\pi S R^2 \sin^2\beta \tag{5}$$

where β is the half-filling angle. For small β, and taking the dimensionless form, this expression may be written as

$$V^* = 2\pi S^* \beta^2 \tag{6}$$

where $S^* = S/R$ and is the dimensionless half-separation distance between the spheres. From eq 4, the radius of curvature, $\bar{r}$, of the bridge surface can be estimated from the geometry at the neck:

$$\frac{1}{\bar{r}} = \frac{1}{R\beta} - \frac{1}{S} \tag{7}$$

For half-separation distances much less than the neck radius, $S \ll R\beta$ and $\bar{r} \approx -S$; hence, the hydrostatic pressure difference from the Laplace−Young equation is

$$\Delta P = -\frac{\gamma}{S} \tag{8}$$

In addition, if $S \ll R\beta$ (or from eq 5, in terms of the bridge volume, if $V/S^3 = V^*/S^{*3} \gg 1$), then the attractive force is dominated by the reduced pressure contribution and hence, from eq 3, the total force of attraction is given by

$$F = \frac{\gamma}{S}\pi R^2 \beta^2 \tag{9}$$

In dimensionless form this becomes

$$F^* = \frac{\beta^2}{2S^*} \tag{10}$$

where F^* $(= F/2\pi R\gamma)$ is the dimensionless attractive force. From eqs 10 and 6, we obtain

$$4\pi F^* = \left(\frac{\sqrt{V^*}}{S^*}\right)^2 = \left(\frac{1}{S^+}\right)^2 = \left(\frac{L}{S}\right)^2 \tag{11}$$

where $S^+ (= S^*/V^{*1/2} = S/L)$ is a scaled dimensionless half-separation distance and L $(= (V/R)^{1/2})$ is a characteristic length for the problem. The dimensionless force is, to a first approximation, only a function of S^+.

Figure 5a shows a dimensionless plot of the attractive force between equal spheres as a function of the separation distance calculated using eq 3 for a range of bridge volumes and a solid−liquid contact angle of zero. A similar plot is shown in Figure 5b except that the force is plotted as a function of S^+, which provides a reasonable superposition of the curves in Figure 5a, as predicted by eq 11. The quality of this superposition deteriorates with increasing contact angle, as is shown in Figure 5d for a contact angle of 40°.

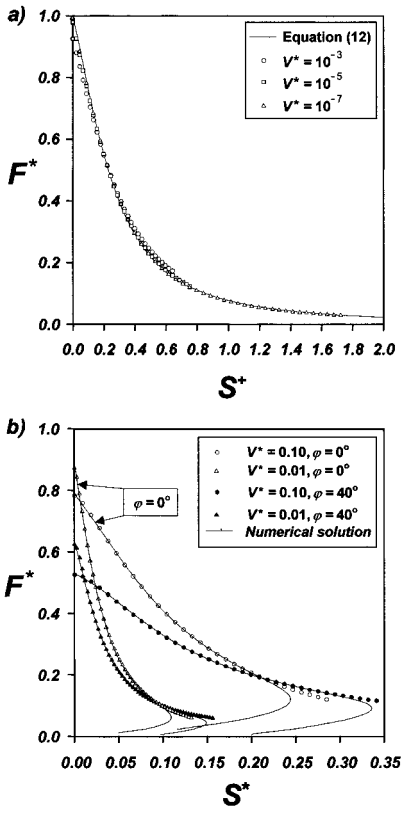

Figure 6. Dimensionless plots of the total capillary force as a function of the separation distance between equal spheres for a range of dimensionless liquid bridge volumes. The points in (a) were calculated by numerical solution of the Laplace−Young equation and using eq 3, the curve using the closed-form approximation given by eq 12; a contact angle of zero was used in both cases. The points in (b) were calculated using the closed-form approximation given by eq A1, the curves by numerical solution of the Laplace−Young equation and using eq 3; contact angles of either zero or 40° were used in both cases.

The curves in Figure 5b for a contact angle of zero are indistinguishable for dimensionless volumes of $<10^{-5}$; this is also found to be the case for any contact angle. The following polynomial in S^+ was the best fit for $V^* = 10^{-7}$:

$$F^* = \frac{\cos\varphi}{1 + 2.1(S^+) + 10.0(S^+)^2} \tag{12}$$

which provides a closed-form approximation for the total capillary forces between equal spheres as a function of the separation distance and for a fixed bridge volume. The accuracy of this expression is exemplified in Figure 6a, where the exact results are compared to the approximate values. The errors increase with increasing volume. However, the maximum error for any contact angle is 4% for $V^* = 0.001$, which corresponds to a filling angle, 2β, of about 20°.

A considerably more complex expression is required for greater volumes and contact angles, and this is given in the Appendix. The expression is valid for $\varphi < 50°$ and $V^* < 0.1$ and gives an error in the force estimate of less than

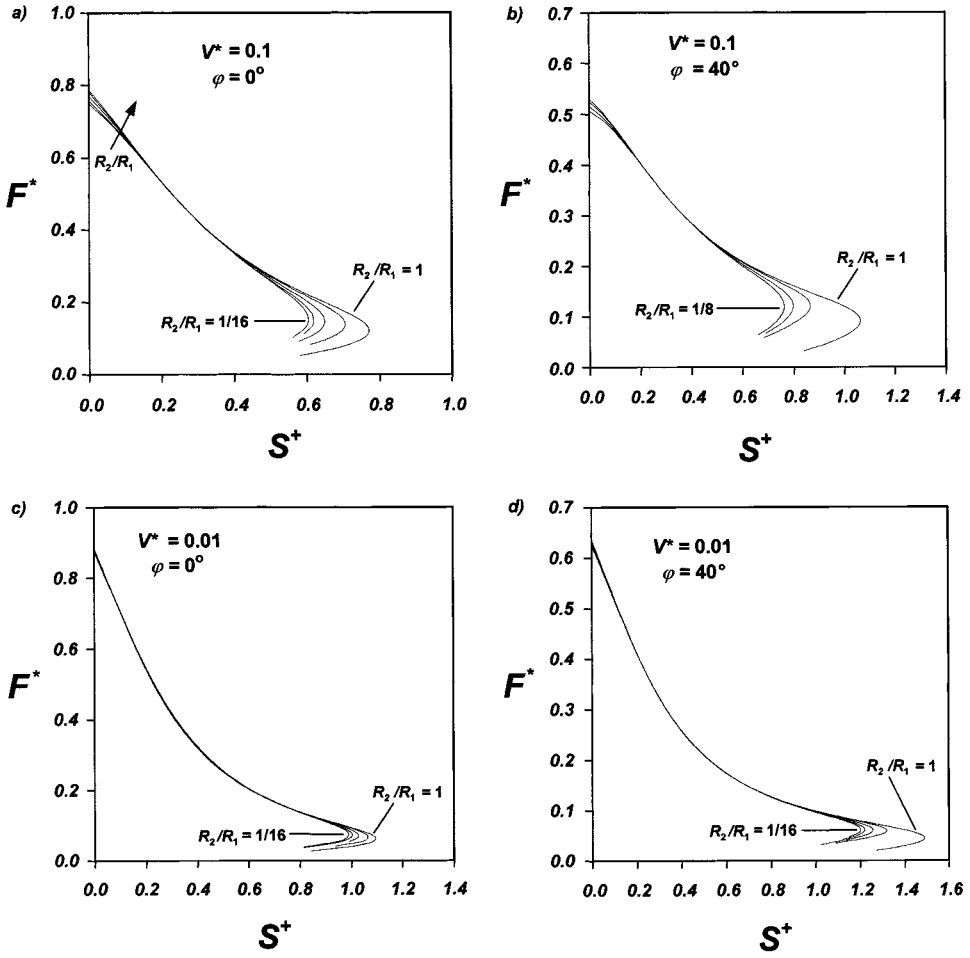

Figure 7. Dimensionless plots of the total capillary force as a function of the separation distance, calculated by numerical solution of the Laplace−Young equation and using eq 3, for spheres with the following radius ratios: 1, 1/2, 1/4, 1/8, and 1/16. The dimensionless liquid bridge volumes and contact angles used in the calculations are shown in the figures.

3%. This is exemplified in Figure 6b, which shows a comparison of the approximate and exact results for a pair of contact angles and bridge volumes.

Derjaguin Approximation for Capillary Forces between Unequal Spheres. In the Introduction, it was pointed out that the capillary forces for unequal spheres may be estimated from the equal sphere toroidal approximation by using the Derjaguin radius, $R_{1,2}$ (eq 1).

In the remainder of this section, all dimensionless quantities containing the sphere radius, R, (i.e., F^*, S^*, V^*, and S^+) will be replaced by the Derjaguin radius to identify the errors involved with this approach. Figure 7 shows dimensionless plots of the total capillary force as a function of the separation distance values calculated by numerical solution of the Laplace−Young equation, using eq 3 for spheres having equal and unequal radii and for different bridge volumes and contact angles. The coincidence of the curves for spheres having different radius ratios demonstrates that the total capillary force for a liquid bridge between a pair of unequal spheres (with radii R_1 and R_2) is indeed close to that calculated for a pair of equal spheres having the Derjaguin radius, $R_{1,2}$, of the pair (eq 1). This also means that the accurate closed-form approximation for equal spheres given in eq A1 can be used to calculate the total capillary force for unequal spheres by appropriate substitution of the Derjaguin radius. Deviations from the solutions for equal spheres occur only when the bridge volume is large compared to those of the spheres and at small and large separation distances. More specifically, if the dimensionless volume, V^*, is less than 0.01, the errors are <2% for a zero separation (becoming less for smaller volumes), decreasing to near zero at intermediate separations, with a steady over-prediction of the force at separations approaching the rupture distance. The error at large separations results in an over-prediction of bridge rupture distances.

As another example of the use of the Derjaguin approximation, an equation derived by Israelachvili[20] for the attractive force between a sphere of radius R_1 with a flat ($1/R_2 = 0$) may be expressed in terms of the Derjaguin radius:

$$F^* = \frac{F}{2\pi R_{1,2}\gamma} = \frac{R_{1,2}(1 - \cos\beta)\cos\varphi}{R_{1,2}(1 - \cos\beta) + 2S} \qquad (13)$$

It should be noted that although this simple expression is accurate in the limit of small separation distances and filling angles, it is significantly less accurate than eq 12 at finite values. This is exemplified in Figure 8 for the case of a liquid bridge between a sphere and a flat. In addition, the use of eq 13 is also dependent on a knowledge of the geometric parameter β, which is frequently not known or accessible in real cases.

The Derjaguin approximation was originally derived for determining the force law between unequal spheres on the basis of the interaction energy between planar surfaces.[20] There are no restrictions on the nature of the law, but the validity is assumed to be limited to separation distances that are small compared to the radii of the

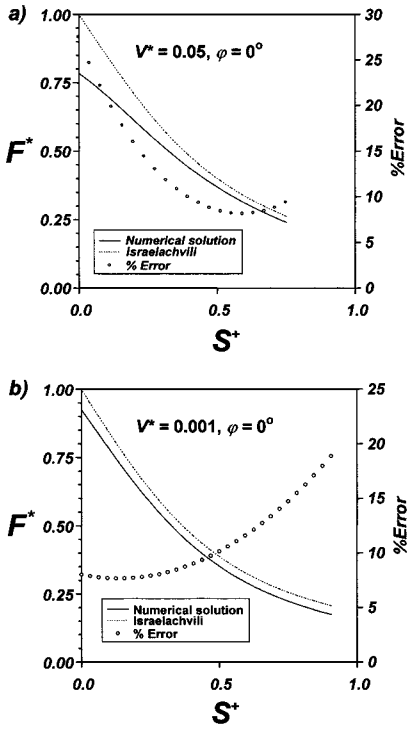

Figure 8. A comparison of the Israelachvili approximation (eq 13) with the numerical solution to the Laplace−Young equation and using eq 3 for a sphere on a flat, a zero contact angle, and dimensionless liquid bridge volumes of (a) 0.05 and (b) 0.001.

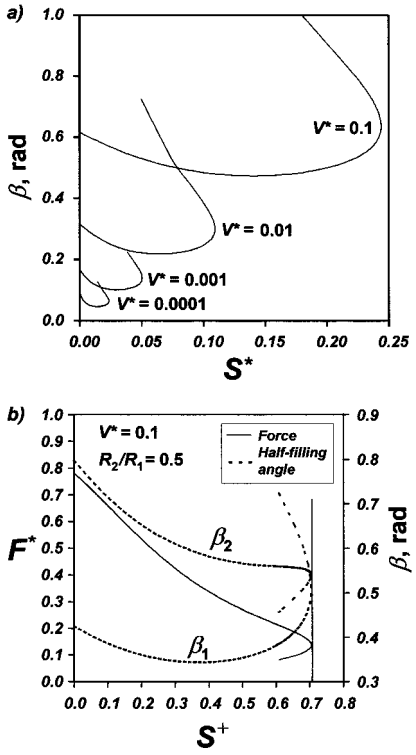

Figure 9. (a) The variation in the bridge half-filling angle as a function of the separation distance, calculated from constant surface-curvature numerical solutions of the bridge profiles between equal spheres, for a contact angle of zero and the different liquid bridge volumes shown. (b) The total capillary force and half-filling angle as a function of the separation distance, calculated by numerical solution of the Laplace−Young equation for unequal spheres with a radius ratio of 1/2, a dimensionless liquid bridge volume of 0.1, and a contact angle of zero.

spheres. The derivation is based on the parabolic approximation of the geometry of the spheres and hence, for pendular liquid bridges, it might be expected that the approximation is most accurate for small filling angles rather than for close contact. There is some evidence from the calculated filling angles to support this contention; the filling angle for equal spheres is a maximum at close contact and near the point of rupture, and this is shown in Figure 9a. Moreover, the error at close separation is increased by large bridge volumes. In addition, for relatively large size ratios there is a tendency for the filling angle on the smaller sphere, β_2, at close separation to be greater than for equal spheres; this increase is shown in Figure 9b. The bridge filling angle decreases as the particles are separated, giving a higher accuracy at intermediate separation distances. Once the filling angle begins to increase near the point of rupture, error is again incurred.

Rupture Distance. The measured rupture distances for the sphere−flat combination were overestimated by eq 2, which is an approximation of the exact result for equal spheres. This is more clearly demonstrated in Figure 3 by the exact values calculated for three size ratios. The results of more detailed calculations are shown in Figure 10 for contact angles of zero and 40°. The following expression is a better approximation of the best-fit equation to these data:

$$2S_c^* = \left(1 + \frac{\varphi}{4}\left(\frac{R_2}{R_1} + 1\right)\right)\left[V^{*1/3} + \left(\frac{R_2}{2R_1} - \frac{2}{5}\right)V^{*2/3}\right] \quad (14)$$

The accuracy of this expression is evident from Figure 10, which shows a comparison of the results calculated on this basis and the exact results from eq 3. For equal spheres, the approximation reduces to

$$2S_c^* = \left(1 + \frac{\varphi}{2}\right)\left(V^{*1/3} + \frac{V^{*2/3}}{10}\right) \quad (15)$$

which predicts a slightly greater rupture distance than eq 2.

Conclusions

The experimental technique described in the current paper is capable of accurately measuring the capillary force−separation characteristics of small pendular liquid bridges between spherical bodies. The accuracy was verified by calculations of the theoretical values that neglect the influence of the disjoining pressure and gravity. That the experimental data are accurately described by these calculations supports the contention of Gao[1,12] that the effect of the film pressure is small for systems involving spherical solids. The negligible influence of gravity was not consistent in all cases with the criteria proposed previously.[25,28] However, there is some evidence to suggest that such criteria are unnecessarily restrictive.[28]

Both theory and experiment show a monotonic decay in the capillary force as the separation distance was increased, and no reduction near the point of zero separation was observed that has been a characteristic of some reported data.[19,22,25]

A scaling method was introduced in order to allow the force−separation curves for equal spheres at different bridge volumes to be superimposed. The scaling coefficient is a characteristic system length L (= $(V/R)^{1/2}$), and the

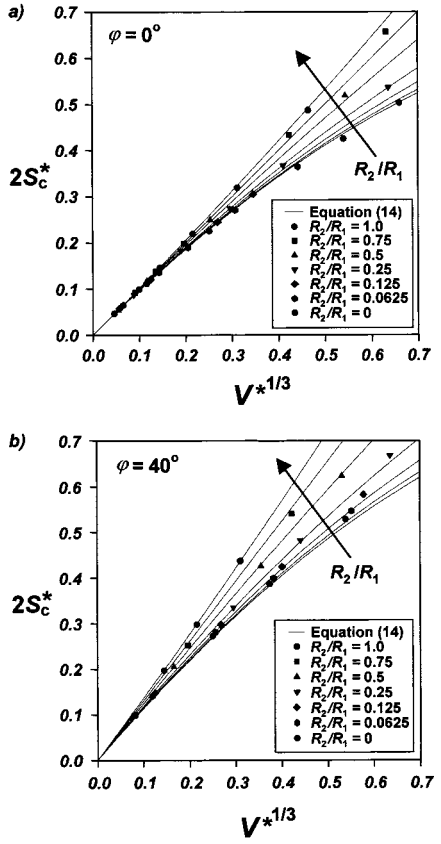

Figure 10. The points are dimensionless rupture distances as a function of the dimensionless liquid bridge volume, calculated by numerical solution of the Laplace−Young equation, for a range of unequal sphere sizes and contact angles of (a) zero and (b) 40°. The curves are calculated using the approximate relationship given by eq 14.

method leads to the development of accurate closed-form expressions for the force as a function of the separation distance for a given bridge volume and contact angle. The accuracy of the Derjaguin approximation for extending the method to spheres of unequal size was assessed. It was shown that rather than being applicable to small separations as argued previously, the error is minimized when the filling angles are small or the dimensionless bridge volume is <0.01; that is, the approximation is relatively accurate over the full range of separation distances except at close contact and near the rupture distance when the filling angle on at least one of the spheres shows a maximum value. The rupture distance for a given quantity of liquid has been shown to be less for a pair of unequal spheres than for a pair of equal spheres possessing the Derjaguin radius of the unequal pair. The extent of the decrease in the rupture distances has also been predicted by the numerical method, and a simple approximate relationship has been proposed.

Appendix

The following expression may be used to calculate the total capillary forces as a function of separation distance for a given contact angle and bridge volume. It was derived by curve-fitting to the numerical solution:

$$\ln F^* = f_1 - f_2 \exp(f_3 \ln S^+ + f_4 \ln^2 S^+) \quad \text{(A1)}$$

where

$$f_1 = (-0.44507 + 0.050832\varphi - 1.1466\varphi^2) + (-0.1119 - 0.000411\varphi - 0.1490\varphi^2) \ln V^* + (-0.012101 - 0.0036456\varphi - 0.01255\varphi^2)(\ln V^*)^2 + (-0.0005 - 0.0003505\varphi - 0.00029076\varphi^2)(\ln V^*)^3$$

$$f_2 = (1.9222 - 0.57473\varphi - 1.2918\varphi^2) + (-0.0668 - 0.1201\varphi - 0.22574\varphi^2)\ln V^* + (-0.0013375 - 0.0068988\varphi - 0.01137\varphi^2)(\ln V^*)^2$$

$$f_3 = (1.268 - 0.01396\varphi - 0.23566\varphi^2) + (0.198 + 0.092\varphi - 0.06418\varphi^2)\ln V^* + (0.02232 + 0.02238\varphi - 0.009853\varphi^2)(\ln V^*)^2 + (0.0008585 + 0.001318\varphi - 0.00053\varphi^2)(\ln V^*)^3$$

$$f_4 = (-0.010703 + 0.073776\varphi - 0.34742\varphi^2) + (0.03345 + 0.04543\varphi - 0.09056\varphi^2)\ln V^* + (0.0018574 + 0.004456\varphi - 0.006257\varphi^2)(\ln V^*)^2$$

which is valid for $\varphi < 50°$ and $V^* < 0.1$ and gives an error in the force estimate of less than 3%.

LA000657Y